Sequential Tyrosine Sulfation of CXCR4 by Tyrosylprotein Sulfotransferases[†]

Christoph Seibert,*[,‡] Christopher T. Veldkamp,[§] Francis C. Peterson,[§] Brian T. Chait,[||] Brian F. Volkman,[§] and Thomas P. Sakmar[‡]

Laboratory of Molecular Biology and Biochemistry and Laboratory for Mass Spectrometry and Gaseous Ion Chemistry, The Rockefeller University, New York, New York 10065, and Department of Biochemistry, Medical College of Wisconsin, Milwaukee, Wisconsin 53226

Received May 21, 2008; Revised Manuscript Received August 27, 2008

ABSTRACT: CXC-chemokine receptor 4 (CXCR4) is a G protein-coupled receptor for stromal cell-derived factor-1 (SDF-1/CXCL12). SDF-1-induced CXCR4 signaling is indispensable for embryonic development and crucial for immune cell homing and has been implicated in metastasis of numerous types of cancer. CXCR4 also serves as the major coreceptor for cellular entry of T-cell line-tropic (X4) HIV-1 strains. Tyrosine residues in the N-terminal tail of CXCR4, which are post-translationally sulfated, are implicated in the high-affinity binding of SDF-1 to CXCR4. However, the specific roles of three potential tyrosine sulfation sites are not well understood. We investigated the pattern and sequence of CXCR4 sulfation by using recombinant human tyrosylprotein sulfotransferases TPST-1 and TPST-2 to modify a peptide that corresponds to amino acids 1−38 of the receptor (CXCR4 1−38). We analyzed the reaction products with a combination of reversed-phase HPLC, proteolytic cleavage, and mass spectrometry. We found that CXCR4 1−38 is sulfated efficiently by both TPST enzymes, leading to a final product with three sulfotyrosine residues. Sulfates were added stepwise to the peptide, producing specific intermediates with one or two sulfotyrosines. The pattern of sulfation in these intermediates indicates that with both enzymes Tyr-21 is sulfated first, followed by Tyr-12 or Tyr-7. Using heteronuclear NMR spectroscopy, we demonstrated that the SDF-1 binding affinity of CXCR4 1−38 increases with the number of sulfotyrosines present, which suggests a potential physiological role for sulfation of all three sites in the N-terminus of CXCR4. These results provide a structural basis for understanding the role of post-translational tyrosine sulfation in SDF-1-induced CXCR4 signaling.

CXC-chemokine receptor 4 (CXCR4)[1] is a G protein-coupled receptor (GPCR) for stromal cell-derived factor-1 (SDF-1/CXCL12) (*1*−*3*), which is expressed as two functionally indistinguishable alternative splice variants, SDF-1α and SDF-1*β*. CXCR4 is constitutively expressed in most hematopoietic and many nonhematopoietic cell types (*3*) and mediates SDF-1-induced chemotaxis in immune function and embryonic development (*3*−*5*). By coupling to heterotrimeric G proteins of the G_i subfamily, CXCR4 activates a complex network of intracellular signaling pathways involving various second messenger systems leading to cytoskeletal rearrangements and other cellular responses involved in chemotaxis (*6*).

The physiological importance and the lack of redundancy of the CXCR4/SDF-1 system have been demonstrated by gene knockout studies in mice. Disruption of either the *cxcr4* or *sdf-1* gene proved to be absolutely lethal in the perinatal period due to abnormal vascular and cerebellar development, hematopoiesis, and cardiogenesis (*7*−*9*). Gene disruptions of other chemokine receptor systems in contrast do not cause a lethal phenotype. In the adult, the CXCR4/SDF-1 signaling system directs migration of naïve T-cells to secondary lymph nodes for antigen presentation and mediates stem cell homing to the bone marrow. Furthermore, it has been shown that the SDF-1/CXCR4 signaling system is involved in the metastasis of breast cancer (*10*) and ovarian cancer (*11, 12*) and in brain tumor growth (*13*).

In addition to its physiological function as a chemokine receptor for SDF-1, CXCR4 is also used by HIV-1 as a coreceptor for cellular entry (*5*). Entry of HIV-1 into target cells is mediated by a sequential interaction of the envelope glycoprotein gp120 with CD4 and a chemokine receptor on the cell membrane (*14*). Although many chemokine receptors have been shown to be able to mediate HIV-1 entry in vitro, only CCR5 and CXCR4 are likely to be of major importance in vivo (*15, 16*). CCR5-using HIV-1 strains (R5) are

[†] This work was supported by NIH Grants AI058072 (to B.F.V.) and RR00862 (to B.T.C.) and by a Northwestern Mutual Life fellowship from the Medical College of Wisconsin Cancer Center (to F.C.P.).

* To whom correspondence should be addressed: Box 187, The Rockefeller University, 1230 York Ave., New York, NY 10065. Telephone: (212) 327-8283. Fax: (212) 327-7904. E-mail: seiberc@mail.rockefeller.edu.

[‡] Laboratory of Molecular Biology and Biochemistry, The Rockefeller University.

[§] Medical College of Wisconsin.

[||] Laboratory for Mass Spectrometry and Gaseous Ion Chemistry, The Rockefeller University.

[1] Abbreviations: CCR5, CC-chemokine receptor 5; CXCL12, CXC-chemokine ligand 12; CXCR4, CXC-chemokine receptor 4; ESI MS, electrospray ionization mass spectrometry; G protein, guanine nucleotide-binding regulatory protein; GPCR, G protein-coupled receptor; HIV-1, human immunodeficiency virus type 1; MALDI-TOF MS, matrix-assisted laser desorption ionization time-of-flight mass spectrometry; MS, mass spectrometry; PAPS, 3′-phosphoadenosine 5′-phosphosulfate; PSGL-1, P-selectin glycoprotein ligand-1; RP-HPLC, reversed-phase high-performance liquid chromatography; SDF-1α, stromal cell-derived factor-1α; TPST, tyrosylprotein sulfotransferase.

10.1021/bi800965m CCC: $40.75 © XXXX American Chemical Society

Published on Web 10/04/2008

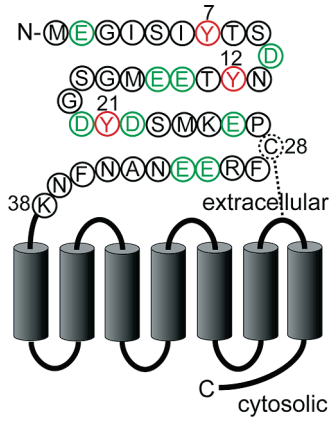

FIGURE 1: Schematic representation of human CXCR4 with potential tyrosine sulfation sites. The seven transmembrane helices are shown as cylinders. Connecting extracellular and cytosolic loops as well as N- and C-terminal regions are depicted as black lines. Amino acid residues in the N-terminus of CXCR4 are represented in single-letter code. The potentially sulfated tyrosine residues at positions 7, 12, and 21 are highlighted in red, and the acidic amino acid residues Asp-10, Asp-20, Asp-22, Glu-2, Glu-14, Glu-15, Glu-26, Glu-31, and Glu-32 are colored green. Cys-28 (dashed circle) forms a putative disulfide bond (dashed line) with Cys-274 in the third extracellular loop of CXCR4.

responsible for almost all cases of HIV-1 transmission, predominate during the asymptomatic phase of the infection, and are sufficient to cause AIDS (*14, 17, 18*). CXCR4-using viruses, on the other hand, are rarely transmitted between individuals and are normally not predominant during the early years of infection. In many cases, CXCR4-using viruses do not emerge during the entire course of the disease; however, in ~50% of infected individuals, these viruses emerge in the later years of infection. The shift from CCR5- to CXCR4-using viruses generally coincides with the clinical onset of AIDS, and it is believed that the emergence of the more pathogenic CXCR4-using HIV-1 strains contributes to the accelerated depletion of $CD4^+$ T-helper cells (*14, 18*).

Interaction of CXCR4 with SDF-1 involves the N-terminal domain, as well as other extracellular regions of the receptor (*19, 20*) (see Figure 1). According to the widely accepted "two-site, two-step" model for chemokine-induced receptor activation (*21, 22*), the chemokine core first binds the receptor N-terminal domain. This initial docking step is followed by a secondary interaction between the chemokine N-terminus and another receptor site, which triggers receptor activation via selective stabilization of the active receptor conformation. The secondary chemokine binding site is not well defined but most likely includes part of the second extracellular loop (*19*) and possibly transmembrane residues of the receptor. Specific electrostatic interactions between negatively charged side chains in the receptor N-terminus (Figure 1) and basic residues in the chemokine are believed to stabilize the docking complex of CXCR4 and SDF-1 (*19, 23*).

Similar to those of CCR5 and other chemokine receptors, the N-terminus of CXCR4 has been shown to be modified by post-translational sulfation of tyrosine residues (*24*), which increases the overall number of negatively charged side chains in the N-terminus available for such interactions. Furthermore, it has also been shown that tyrosine sulfation of CXCR4 enhances the interaction with SDF-1α (*24*). Interestingly, in contrast to the case with CCR5, tyrosine sulfation of CXCR4 does not seem to be important for the interaction of CXCR4 with HIV-1 gp120-CD4 and for CXCR4-mediated viral entry (*24*).

SDF-1α binding competition studies aimed at elucidating the specific roles of the three potential sulfation sites, Tyr-7, Tyr-12, and Tyr-21 (Figure 1), indicated that a sulfotyrosine at position 21 is directly involved in the binding interaction with SDF-1α (*24*). We recently used NMR spectroscopy to analyze the interaction of SDF-1α with a sulfotyrosine peptide corresponding to the N-terminus of CXCR4. We identified the putative binding site for sulfotyrosine 21 on SDF-1α, which involves Arg-47, suggesting the formation of a salt bridge between sulfotyrosine 21 and Arg-47 (*23*). While these findings establish the direct involvement of sulfotyrosine 21 in the interaction of CXCR4 with SDF-1α, the role of Tyr-7 and Tyr-12 remains unclear. On the one hand, metabolic labeling studies indicate that in heterologously overexpressed CXCR4 mutants Tyr-7 and Tyr-12 are sulfated inefficiently (*24*). However, it is not clear whether Tyr-7 and Tyr-12 are sulfated more efficiently in the physiological context of cells that naturally express wild-type CXCR4. In a previous study (*25*), we defined the pattern and sequence of tyrosine sulfation of a peptide corresponding to the N-terminus of CCR5 by using an in vitro sulfation approach and purified recombinant human tyrosylprotein sulfotransferases TPST-1 (*26*) and TPST-2 (*27*).

Here we report a detailed analysis of the in vitro sulfation reaction of a peptide corresponding to amino acids 1−38 of CXCR4 (CXR4 1−38) (Figure 2A). We analyzed intermediates and the final product of the sulfation reaction by using a combination of RP-HPLC, proteolytic cleavage, and mass spectrometry. We found that CXCR4 1−38 is sulfated at similar overall rates by TPST-1 and TPST-2, giving rise to identical intermediates and resulting in a final product in which all three tyrosine residues are sulfated. We also found that sulfates are added stepwise to the peptide and that Tyr-21 is sulfated first, followed by Tyr-12 or Tyr-7. Using heteronuclear NMR spectroscopy, we demonstrated that the binding affinity of the N-terminus of CXCR4 for SDF-1α increases with the number of sulfotyrosines present, indicating a potential physiological role for tyrosine sulfation of all three sites in the CXCR4 N-terminus. These results provide a basis for understanding the role of post-translational tyrosine sulfation in SDF-1α-induced CXCR4 signaling.

MATERIALS AND METHODS

Cells, Plasmids, and Reagents. Expression vectors pMSH1TH and pMSH2TH encoding recombinant engineered human TPST-1 and TPST-2 were a gift from K. L. Moore (University of Oklahoma Health Sciences Center, Oklahoma City, OK). HEK293-T cells were obtained from the American Type Culture Collection (ATCC, Manassas, VA), and cell culture media and supplements were from Invitrogen (Carlsbad, CA). Anti-protein C resin and sequencing-grade endoproteinase Asp-N were obtained from Roche Applied Science (Indianapolis, IN). 3′-Phosphoadenosine 5′-phosphosulfate (PAPS) was from Calbiochem/EMD Biosciences (La Jolla, CA). All other reagents were of the highest grade available and from Sigma-Aldrich (St. Louis, MO) or Fisher Scientific (Pittsburgh, PA).

Analysis and Purification of PAPS. Commercially available PAPS (3′-phosphoadenosine 5′-phosphosulfate) (Calbiochem/

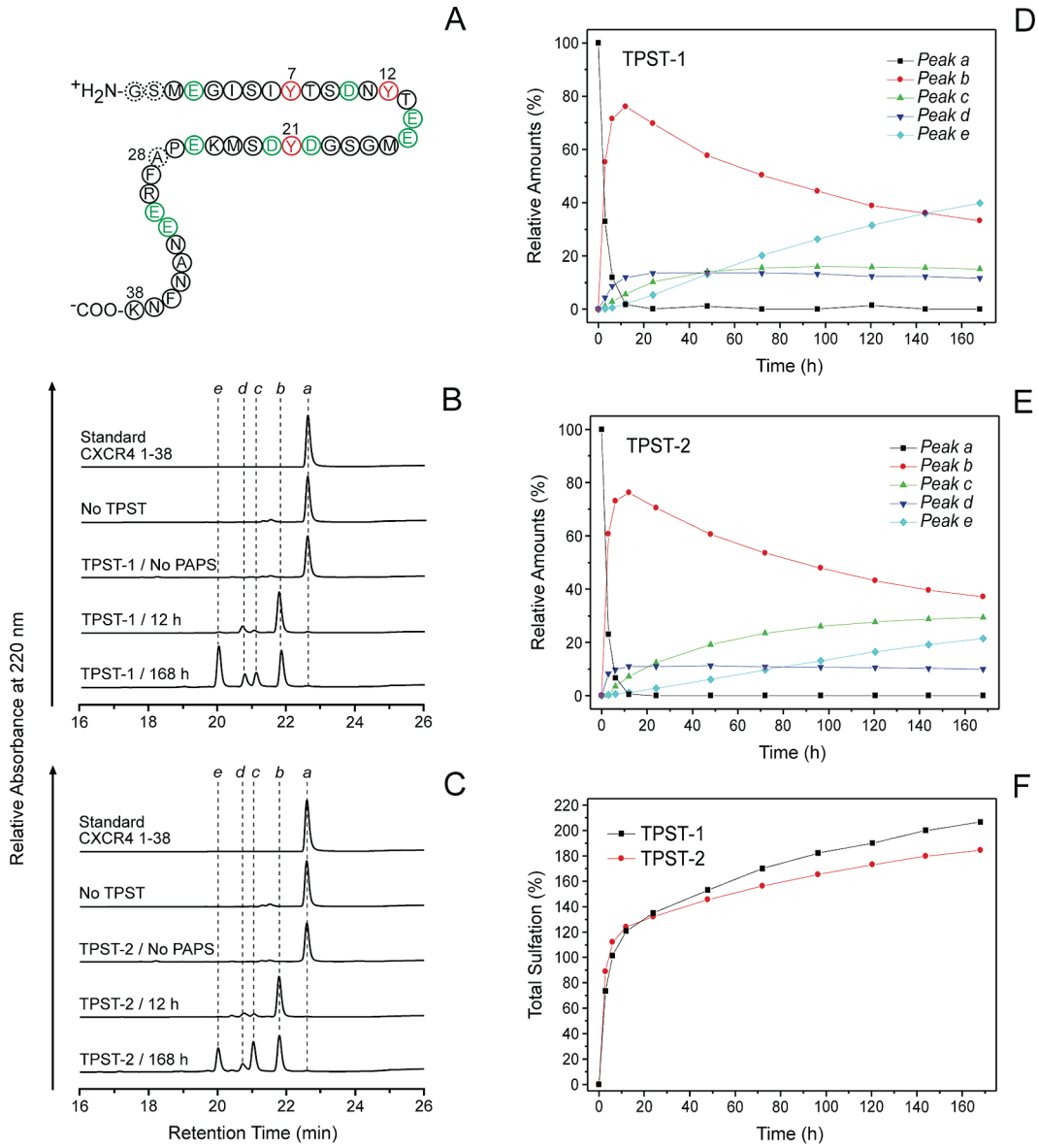

FIGURE 2: TPST-catalyzed in vitro sulfation of CXCR4 1−38. (A) Schematic representation of the sequence of peptide CXCR4 1−38. The color coding is the same as in Figure 1. Ala-28 which replaces Cys-28 of the CXCR4 sequence and the two N-terminal Gly and Ser residues which are not part of the CXCR4 sequence are marked with dashed circles. (B) RP-HPLC analysis of TPST-1-catalyzed CXCR4 1−38 sulfation. Peptide CXCR4 1−38 (50 μM, ≈0.23 mg/mL) was incubated with TPST-1 (40 μg/mL) and in the presence of the sulfotransfer cosubstrate PAPS (400 μM). After 12 or 168 h at 16 °C, 50 μL aliquots were analyzed by RP-HPLC. In negative-control experiments (incubation time of 168 h), either TPST-1 (No TPST) or PAPS (No PAPS) was omitted. As a standard, unreacted CXCR4 1−38 substrate was analyzed. Peaks are labeled a−e in increasing order of hydrophilicity. To correct for day-to-day variations in elution times caused by slight variations in the eluent compositions, elution times were normalized to the average elution time observed for an unsulfated CXCR4 1−38 standard. (C) RP-HPLC analysis of TPST-2-catalyzed CXCR4 1−38 sulfation. Peptide CXCR4 1−38 (50 μM, ≈0.23 mg/mL) was incubated with TPST-2 (40 μg/mL) as described for TPST-1 in panel B. (D) Time course of TPST-1-catalyzed CXCR4 1−38 sulfation. CXCR4 1−38 (50 μM, ≈0.23 mg/mL) was incubated at 16 °C with PAPS (400 μM) and TPST-1 (40 μg/mL). At the indicated time points, 50 μL aliquots were analyzed by RP-HPLC and relative amounts for the different peptide species (a−e) were calculated from the peak areas at 220 nm. (E) Time course of TPST-2-catalyzed CXCR4 1−38 sulfation. Analysis was performed as described for panel D with TPST-2 (40 μg/mL) as the sulfotransfer enzyme. (F) Total incorporation of sulfate into CXCR4 1−38 by TPST-1 vs TPST-2 calculated as the sum of the relative amounts of all peptide species in panels D and E multiplied by the number of sulfotyrosines present in each peptide species (see Table 1). A value of 100% total sulfation corresponds to a net incorporation of 1 equiv of sulfate per equivalent of CXCR4 1−38; the maximum total sulfate incorporation would be 300%, corresponding to complete sulfation of all three sulfation sites present in the peptide.

EMD Biosciences) was estimated to be ≈80% pure by ion-pair RP-HPLC with UV detection at 260 nm (modified after the method in ref*28*). For some experiments, PAPS was further purified by anion-exchange chromatography using a Mono Q column (GE Healthcare, Piscataway, NJ) to remove 3′-phosphoadenosine 5′-phosphate (PAP) and other impurities (*29*). Concentrations of PAPS stock solutions in water (3−4 mM) were precisely determined by UV spectroscopy using a molar extinction coefficient of 15400 M^{-1} cm^{-1} (at 259 nm and pH 7.0) (*30*).

Expression and Purification of Recombinant Engineered Human TPSTs. Human TPST-1 and TPST-2 were expressed as soluble variants (residues 25−370 and 25−377 of full-length TPST-1 and TPST-2, respectively) lacking the cytoplasmic N-terminus and the transmembrane domain, which are not required for enzymatic activity. A transferrin signal

Table 1: Mass Spectrometry of Sulfation Products[a]

peak	MS label	MALDI-TOF MS	ESI MS	no. of sulfates
a	0	$[(CXCR4\ 1-38) - H]^-$	$[(CXCR4\ 1-38) - 3H]^{3-}$	0
		$[(CXCR4\ 1-38) - 2H]^{2-}$	$[(CXCR4\ 1-38) - 4H]^{4-}$	
b	1	$[(CXCR4\ 1-38 + SO_3) - H]^-$	$[(CXCR4\ 1-38 + SO_3) - 3H]^{3-}$	1
		$[(CXCR4\ 1-38 + SO_3) - 2H]^{2-}$	$[(CXCR4\ 1-38 + SO_3) - 4H]^{4-}$	
c	2	$[(CXCR4\ 1-38 + 2SO_3) - H]^-$	$[(CXCR4\ 1-38 + 2SO_3) - 3H]^{3-}$	2
		$[(CXCR4\ 1-38 + 2SO_3) - 2H]^{2-}$	$[(CXCR4\ 1-38 + 2SO_3) - 4H]^{4-}$	
d[b]	2	$[(CXCR4\ 1-38 + 2SO_3) - H]^-$	$[(CXCR4\ 1-38 + 2SO_3) - 3H]^{3-}$	2
		$[(CXCR4\ 1-38 + 2SO_3) - 2H]^{2-}$	$[(CXCR4\ 1-38 + 2SO_3) - 4H]^{4-}$	
e	3	$[(CXCR4\ 1-38 + 3SO_3) - H]^-$	$[(CXCR4\ 1-38 + 3SO_3) - 3H]^{3-}$	3
		$[(CXCR4\ 1-38 + 3SO_3) - 2H]^{2-}$	$[(CXCR4\ 1-38 + 3SO_3) - 4H]^{4-}$	

[a] Sulfation products purified by RP-HPLC were analyzed by MALDI-TOF MS and ESI MS. [b] If DTT was absent during the sulfation reaction, a monosulfated and mono-oxidized CXCR4 1−38 species was found as a minor component in peak d (data not shown).

peptide followed by a protein C epitope was N-terminally fused to the catalytic domain of both TPSTs (*27*). TPST expression and purification were conducted as described previously (*25*). HEK293-T cells were transfected with plasmid pMSH1TH or pMSH2TH using LipofectAMINE Plus (Invitrogen). After 48 h, plates were washed once with PBS and cells were harvested in ice-cold PBS supplemented with the protease inhibitor cocktail Complete (Roche Applied Science). TPSTs were purified from HEK293-T cell extracts by anti-protein C immunoaffinity chromatography (*26*). Purified TPSTs were then concentrated using Centricon YM-10 concentrators (Millipore, Bedford, MA), quantified by densitometry of Coomassie Blue R-250-stained SDS−PAGE gels using BSA (Pierce, Rockford, IL) as a protein standard, and stored at −80 °C in elution buffer [20 mM MOPS (pH 7.5), 150 mM NaCl, 10 mM EDTA, 0.1% (w/v) Triton X-100, and 10% (w/v) glycerol]. The enzymatic activity of the purified TPSTs was tested using the PSGL-1 1−15 peptide (amino acids 1−15 of the P-selectin glycoprotein ligand-1, QATEYEYLDYDFLPE-NH_2) as a substrate.

Expression and Purification of an N-Terminal CXCR4 Peptide. Peptide CXCR4 1−38 was expressed in *Escherichia coli* as a fusion protein with an N-terminal hexahistidine tag followed by the Ig-binding domain of protein G and a tobacco etch virus (TEV) protease cleavage site (*23*). To prevent dimerization through cysteine oxidation, Cys-28 of CXCR4 was replaced with alanine. Removal of the N-terminal fusion protein by TEV protease cleavage resulted in a CXCR4 1−38 peptide, which contained an additional Gly-Ser dipeptide at its N-terminus that is not present in the CXCR4 sequence (Figure 2A). Expression and purification of the peptide according to published procedures (*23*) gave a product of >98% homogeneity as judged by analytical RP-HPLC.

In Vitro Sulfation of CXCR4 1−38. Stock solutions of CXCR4 1−38 at 2 mM were prepared in H_2O and neutralized with NaOH. Peptide concentrations were measured by UV absorption at a wavelength of 280 nm using a calculated extinction coefficient (ϵ) of 3840 cm^{-1} M^{-1} (http://us.expasy.org/tools/protparam.html). In vitro sulfation was conducted as described previously (*25*) using reaction conditions that were optimized for efficient sulfation of CXCR4 1−38. CXCR4 1−38 was diluted in sulfation buffer [40 mM PIPES (pH 6.8), 100 mM NaCl, and 0.1% Triton X-100] (*27*) to a final concentration of 50 μM (≈0.23 mg/mL), and 10 mM DTT was added for TPST-1-catalyzed reactions. TPST-1 or TPST-2 (40 μg/mL) and the sulfotransfer cosubstrate PAPS (400 μM) were added, and the reaction mixtures were incubated at 16 °C. At selected time points, aliquots of the sulfation reactions were removed and analyzed by RP-HPLC and MS. To prepare milligram quantities of CXCR4 1−38 sulfotyrosine peptides for binding experiments, 100−200 μg/mL TPST-1 was used in large-scale sulfation reactions.

RP-HPLC of Sulfotyrosine Peptides. Prior to RP-HPLC analysis, sample cleanup was performed by extraction with a 2:1 (v/v) mixture of chloroform and methanol followed by solid-phase extraction using Bio-Select C18 columns (218SPE3000; Grace Vydac, Hesperia, CA). Samples were analyzed on an analytical C18 column [218TP54, 5 μm, 300 Å (Grace Vydac)] with UV detection at 220 nm. Sulfopeptide separation was achieved with a linear gradient from 5 to 60% eluent B over 40 min at a flow rate of 1.0 mL/min [eluent A, 20 mM ammonium acetate (pH 6.5) in water; eluent B, 20 mM ammonium acetate (pH 6.5) in 70% acetonitrile]. For analytical separations, 50 μL samples were injected and eluting fractions corresponding to peptide peaks were collected. For mass spectrometry analysis, solvent was evaporated, samples were redissolved in 150 μL of a 1:2 (v/v) mixture of water and acetonitrile, and the solvent was evaporated again to remove residual ammonium acetate. To purify milligram quantities of sulfotyrosine peptides for binding experiments, samples were purified using a semipreparative C18 column [218TP510 (Grace Vydac)] using a linear gradient from 19 to 30% eluent B over 40 min at a flow rate of 3.0 mL/min. To prevent oxidation of the three methionine residues (Met-1, -16, and -24) in the sulfotyrosine peptides (Figure 2A) throughout the sample preparation, all solvent removal steps were performed either by lyophilization or by using a Speed Vac vacuum concentrator (Thermo Scientific Savant, Waltham, MA) that was set up in a cold room and operated at a low temperature setting.

Mass Spectrometry. Matrix-assisted laser desorption ionization time-of-flight mass spectrometry (MALDI-TOF MS) of sulfotyrosine peptide samples was conducted as described previously (*25*) using α-cyano-4-hydroxycinnamic acid (Sigma) as a matrix. Solvent conditions were optimized to prevent disruption of labile thioester bonds. The matrix was prepared as a saturated solution in a 2:1 (v/v) mixture of water and acetonitrile with 10 mM ammonium acetate as an additive. Samples were diluted 1:10 in matrix solution, and a small aliquot (1 μL) of peptide matrix solution was spotted onto the sample plate using an ultrathin layer method (*31*). For some experiments, samples were spotted using the dried droplet method (*32, 33*). To prevent sodium adduct formation

and to stabilize sulfotyrosine residues, samples were prepared in the presence of 10 mM ammonium acetate and spots were washed once with 1.5 μL of an ice-cold 5 M ammonium acetate solution. MALDI-TOF mass measurements were performed on a Voyager DE-STR instrument (Applied Biosystems, Foster City, CA), operating in negative linear, delayed extraction mode. For each measurement, spectra from 100 individual laser shots were averaged (2 ns data channel width).

Electrospray ionization (ESI) mass measurements were performed on a QSTAR XL hybrid electrospray quadrupole−quadrupole time-of-flight mass spectrometer (Applied Biosystems). Peptide samples were desalted by binding to reversed-phase C18 ZipTips (Millipore, Billerica, MA). After being washed with deionized water, peptides were eluted with 70% acetonitrile and the peptide solutions were injected into the nanoelectrospray ionization source of the mass spectrometer using PicoTip emitters (New Objective Inc., Woburn, MA) at a flow rate of approximately 20 nL/min. ESI mass spectra were recorded in negative ion TOF MS mode at an electrospray potential of −1.4 kV with a declustering potential of −55 V.

Mass spectra obtained by MALDI-TOF MS and ESI MS were calibrated externally and internally and further analyzed using M-over-Z (http://bioinformatics.genomicsolutions.com). Theoretical peptide masses were determined using paws (http://bioinformatics.genomicsolutions.com).

Endoproteinase Asp-N Cleavage of Sulfotyrosine Peptides. HPLC-purified sulfotyrosine peptides (0.1−1 μg) were dissolved in 10 μL of a 40 mM ammonium acetate solution (pH 8.0). Endoproteinase Asp-N (2 ng/μL) was added, and the mixtures were incubated at room temperature. At selected time points (2 and 18 h), aliquots (5 μL) of the cleavage reaction were removed and dried using a vacuum concentrator. Samples were dissolved in a small volume (3 μL) of a saturated α-cyano-4-hydroxycinnamic acid matrix solution and analyzed by MALDI-TOF MS as described.

Determination of SDF-1α Peptide Binding Affinities by Heteronuclear NMR Spectroscopy. NMR chemical shift assignments of SDF-1α have been described previously (*22, 34, 35*). Titrations of SDF-1α with unsulfated, Y21-monosulfated, and fully sulfated CXCR4 1−38 peptides were performed as described previously (*23*). Briefly, [U-^{15}N/^{13}C]SDF-1α (50 μM) in 20 mM MES (pH 6.8) was titrated with incremental additions of the peptides and monitored via one-dimensional (1D) ^{1}H, two-dimensional (2D) ^{15}N−^{1}H HSQC, 2D aliphatic ^{13}C−^{1}H HSQC, and 2D aromatic ^{13}C−^{1}H HSQC spectra. Under these conditions, SDF-1α peptide binding occurs in fast exchange on the chemical shift time scale, allowing most chemical shift assignments to be transferred by inspection. Final amide proton and nitrogen assignments were confirmed using a three-dimensional (3D) HNCA spectrum. Amide ^{1}H−^{15}N chemical shift perturbations were computed as $[(5\Delta\delta_{NH})^2 + (\Delta\delta_N)^2]^{1/2}$, where $\Delta\delta_{NH}$ and $\Delta\delta_N$ are the changes in backbone amide ^{1}H and ^{15}N chemical shifts, respectively, in parts per million. Concentration-dependent changes in amide chemical shift perturbations for SDF-1α residues 23, 25, 29, 31, 40−42, 47−51, 62, and 65−67 upon titration with CXCR4 peptides were fitted to the following equation that accounts for ligand depletion:

$$\Delta\delta = \frac{\Delta\delta_{max}}{2[\text{SDF-1}]} \times \sqrt{K_d + [\text{SDF-1}] + x - (K_d + [\text{SDF-1}] + x)^2 - 4[\text{SDF-1}]x}$$

where $\Delta\delta$ represents the chemical shift perturbation, $\Delta\delta_{max}$ is the maximum chemical shift perturbation at 100% bound SDF-1α, K_d is the apparent SDF-1α peptide dissociation constant, and x is the peptide concentration. K_d and $\Delta\delta_{max}$ values were obtained for each of the aforementioned SDF-1α residues by nonlinear curve fitting. For ease of comparison, the individual $\Delta\delta_{max}$ values were normalized to a value of 1, and the individual K_d values were used to calculate average K_d values and standard deviations for each of the CXCR4 peptides.

RESULTS

Enzymatic in Vitro Sulfation of CXCR4 1−38. To characterize tyrosine sulfation of the N-terminus of CXCR4 (Figure 1), we studied the TPST-catalyzed in vitro sulfation reaction of a peptide corresponding to amino acids 1−38 of CXCR4 (CXCR4 1−38) as a model system (Figure 2A). The CXCR4 1−38 peptide was expressed in *E. coli* as a recombinant fusion protein, and cleavage by TEV protease resulted in an N-terminal Gly-Ser extension, which is not part of the CXCR4 sequence. Furthermore, to prevent oxidative dimerization of the peptide, Cys-28 of CXCR4 was replaced with alanine in CXCR4 1−38 (Figure 2A). In initial experiments, we optimized the reaction conditions for efficient sulfation of CXCR4 1−38 by TPST-1 and TPST-2 using RP-HPLC to analyze time-dependent formation of the reaction products (data not shown). The concentration of the sulfation cosubstrate PAPS (400 μM) was adjusted to allow for stoichiometric sulfation of all three potential sites in the peptide (50 μM), and different TPST concentrations and sulfation buffer compositions were tested at various reaction temperatures. We found that sulfation by TPST-1 was more efficient in the presence of DTT while sulfation by TPST-2 did not benefit from DTT (data not shown). Therefore, we included 10 mM DTT in the sulfation buffer for TPST-1 only. These optimized reaction conditions (see Materials and Methods) gave a reproducibly high level of incorporation of sulfate into the CXCR4 1−38 peptide and were used throughout all the following experiments.

During the course of the sulfation reaction with TPST-1 or TPST-2, five major peptide species (peaks a−e) were identified by RP-HPLC (Figure 2B,C). Peak a, which eluted as the most hydrophobic peptide species, corresponds to the unreacted peptide. Peaks b−e, which represent different products of the sulfation reaction with retention times decreasing in increments of approximately 0.3−0.8 min (Figure 2B,C), appeared in a time-dependent fashion (Figure 2B−E). Using optimized reaction conditions, CXCR4 1−38 sulfation progressed for at least 160 h (Figure 2B−E). In the absence of TPST or PAPS, no sulfation products were seen (Figure 2B,C), indicating specific TPST-catalyzed sulfation. While both TPST-1 and TPST-2 were able to modify CXCR4 1−38 at comparable rates (Figure 2F) and produce similar peak patterns, there were significant and reproducible differences in the relative peak intensities (Figure 2B−E). In particular, peak c was more pronounced with TPST-2 than with TPST-1.

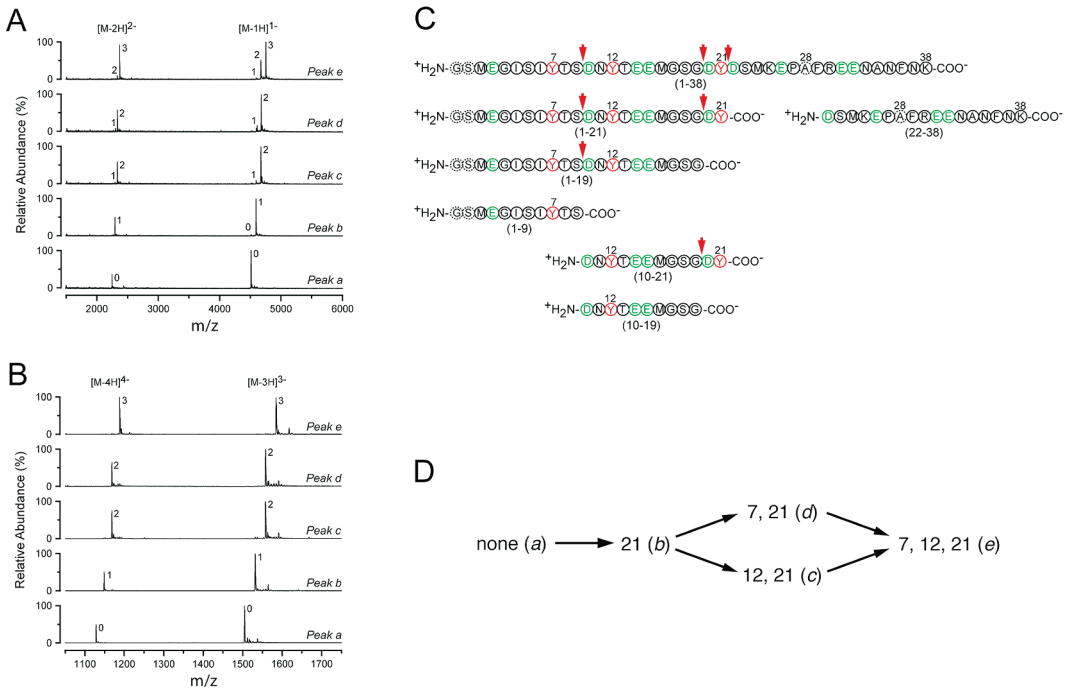

FIGURE 3: Identification of sulfation sites in CXCR4 1−38 sulfation products. Peak fractions a−e from RP-HPLC were analyzed by (A) negative ion mode MALDI-TOF MS and (B) negative ion mode ESI MS. Peaks are labeled according to the number of identified sulfotyrosines as shown in Table 1; satellite peaks corresponding to sodium adducts and oxidation of Met residues are not labeled. In MALDI-TOF MS (A), the dominant peaks in each spectrum correspond to the $[M - 1H]^-$ and $[M - 2H]^{2-}$ ions. Minor peaks indicate the loss of one or two SO_3 groups during MS analysis. In ESI MS (B), the two dominant peaks in each spectrum correspond to the $[M - 3H]^{3-}$ and $[M - 4H]^{4-}$ ions. (C) Schematic representation of peptide fragments generated by Asp-N cleavage that were used to localize sulfation sites in CXCR4 1−38 sulfation products by MALDI-TOF MS analysis. The color coding is the same as in Figure 1, and the endoproteinase Asp-N cleavage sites are denoted with red arrows. The peptide fragments are numbered according to the CXCR4 sequence excluding the N-terminal Gly and Ser extension. Fragments 1−19, 1−21, and 10−21 are intermediates of the cleavage reaction, whereas fragments 1−9, 10−19, and 22−38 emerged as the final cleavage products. (D) Reaction scheme for the sequential sulfation of CXCR4 1−38 by TPST-1 and TPST-2. CXCR4 1−38 species that arise from sulfation of nonsulfated CXCR4 1−38 (none) with either TPST-1 or TPST-2 are represented by their sulfotyrosine positions. The corresponding HPLC peak assignments are given in parentheses.

In addition to the five major sulfation products (peaks a−e), two minor peaks (peaks b′ and d′) were detected during the course of the sulfation reaction. Due to their low abundance, these peaks are barely visible in the HPLC traces in panels B and C of Figure 2 (peak b′ eluted ca. 0.3 min before peak b, and peak d′ eluted ca. 0.3 min before peak d). Preliminary MS analysis indicated that these peaks most likely correspond to methionine-oxidized sulfopeptide species. Methionine oxidation most likely occurred as a side reaction during the in vitro sulfation reaction and/or the sample preparation procedure, because only negligible quantities of oxidized peptide species were observed by mass spectrometry analysis of the unmodified CXCR4 1−38 peptide. Furthermore, the level of methionine oxidation was significantly reduced if DTT (10 mM) was present in the sulfation buffer. Due to their low abundance, we did not attempt to further characterize these side products of the sulfation reaction.

Mass Spectrometry of CXCR4 1−38 Sulfation Products. The formation of several sulfation products with different hydrophilicities indicates that these represent CXCR4 1−38 species that differ in the number or positions of tyrosine sulfates (*25*). To determine the precise number of sulfotyrosines present in each peptide species, we analyzed the HPLC-purified peak fractions for the TPST-1- and TPST-2-catalyzed sulfation reactions by matrix-assisted laser desorption ionization time-of-flight (MALDI-TOF) (Figure 3A) and electrospray ionization (ESI) mass spectrometry (Figure 3B). For the sake of simplicity, only the MS data for sulfotyrosine peptides obtained by TPST-1-catalyzed sulfation of CXCR4 1−38 are shown in panels A and B of Figure 3.

Initially, CXCR4 1−38 peptide species separated by RP-HPLC were analyzed by MALDI-TOF MS as described for similar CCR5 peptides (*25*). Peak fraction a was first analyzed in positive ion reflector mode (monoisotopical mass M_r = 4512.79 Da) and confirmed to be CXCR4 1−38 (theoretical monoisotopical mass M_r = 4512.89 Da). However, the positive ion reflector mode is inappropriate for the analysis of sulfated peptide species because the sulfoester bond is more labile in positive ions than in negative ions and because metastable ions are observed in reflector mode (see ref*36* and references cited therein). Thus, HPLC fractions corresponding to sulfotyrosine peptides were analyzed in linear negative ion mode (*25*). Masses were determined with a precision exceeding 500 ppm, allowing for the unambiguous identification of each MS peak. Fraction a produced a spectrum with a single pair of $[M - H]^-$ and $[M - 2H]^{2-}$ peaks corresponding to nonsulfated CXCR4 1−38 (Figure 3A). Fractions b−e, in contrast, produced spectra that are characterized by series of $[M - H]^-$ and $[M - 2H]^{2-}$ peaks of increasing complexity, which are caused by loss of SO_3 (ΔM_r = 80 Da) to various degrees (Figure 3A). From the peak series in each spectrum, we were able to determine the number of sulfotyrosines present in each HPLC-purified peptide (Table 1).

Table 2: Mass Spectrometry of Endoproteinase Asp-N Cleavage Fragments[a]

peak	uncleaved	endoproteinase	Asp-N[b]	no. of sulfotyrosines
a	1−38	1−9	10−19	0
b	1−38(SO_3)	1−9	10−19	21
c	1−38(SO_3)$_2$	1−9	10−19(SO_3)	12, 21
d[c]	1−38(SO_3)$_2$	1−9(SO_3)	10−19	7, 21
e	1−38(SO_3)$_3$	1−9(SO_3)	10−19(SO_3)	7, 12, 21

[a] Peptide fragments were identified by MALDI-TOF MS of Asp-N cleavage reaction mixtures. [b] Only final cleavage fragments containing potential tyrosine sulfation sites are presented; data for Asp-N cleavage intermediates are not shown. [c] If DTT was absent during the sulfation reaction, a monosulfated and mono-oxidized CXCR4−p38 species was found as a minor component in peak d (data not shown).

To confirm the MALDI-TOF MS data, the CXCR4 1−38 peptide species were reanalyzed by ESI MS in negative ion mode, which is generally less damaging to sulfotyrosine residues than MALDI-TOF MS (see ref*36* and references cited therein). The ESI mass spectra (Figure 3B) are dominated by $[M - 3H]^{3-}$ and $[M - 4H]^{4-}$ ion peaks, which are accompanied by smaller satellite peaks corresponding to sodium adduct formation and oxidation of one or more of the three methionine residues present in CXCR4 1−38. However, no loss-of-SO_3 peaks are observed under these conditions (Figure 3B), allowing for the unambiguous identification of the sulfotyrosine peptide species and confirming the MALDI-TOF MS data (Table 1). Taken together, the MS data show that the major products of the sulfation reaction represent CXCR4 1−38 species with zero (peak a), one (peak b), two (peaks c and d), and three (peak e) sulfotyrosines (Table 1).

Analysis of Sulfation Sites in CXCR4 1−38 Sulfation Products. To localize the sulfation sites within the CXCR4 1−38 sulfation products, we generated peptide fragments containing subsets of the three tyrosine residues (Tyr-7, -12, and -21) by proteolysis with endoproteinase Asp-N (Figure 3C). Analysis of the cleavage reactions was accomplished by MALDI-TOF MS. Due to the presence of three aspartate residues (Asp-10, Asp-20, and Asp-22) in CXCR4 1−38, multiple cleavage fragments were generated by endoproteinase Asp-N in a time-dependent manner (Figure 3C). In particular, fragments 1−19, 1−21, and 10−21 were observed as intermediates of the cleavage reaction, whereas fragments 1−9, 10−19, and 22−38 emerged as the final cleavage products. To obtain information about all three sulfation sites, proteolysis was conducted with various endoproteinase Asp-N concentrations and cleavage reactions were analyzed at different time points (data not shown). Using this strategy, we were able to identify unambiguously all sulfation sites in the four major CXCR4 1−38 sulfation products (peaks a−e) (Table 2). From these results, we conclude that peak b represents CXCR4 1−38 with a single sulfotyrosine at position 21. Peaks c and d correspond to disulfated CXCR4 1−38 with sulfotyrosines at positions 12 and 21 or 7 and 21, respectively. Peak e, as expected for a CXCR4 1−38 species with three sulfotyrosines, is sulfated at positions 7, 12, and 21.

Sequential Sulfation of CXCR4 1−38 by TPST-1 and TPST-2. On the basis of the structures of the observed CXCR4 1−38 sulfation products, we postulate that the sulfation reaction progresses through the observed intermediates in a sequential manner (Figure 3D). To further substantiate the sequential nature of the sulfation reaction and examine the differences between TPST-1 and TPST-2, we analyzed the time course of CXCR4 1−38 sulfation for both enzymes (Figure 2D,E). CXCR4 1−38 was incubated with either TPST-1 or TPST-2 in the presence of PAPS, and at different time points, the sulfation reaction mixtures were analyzed by RP-HPLC. The time-dependent buildup and depletion of sulfation products are shown for TPST-1 in Figure 2D and for TPST-2 in Figure 2E. Because the sulfation reactions were performed with an excess of peptide substrate over enzyme, the observed kinetics and amounts of intermediates show that the substrate has to be released after each sulfation step (*25*).

In the course of the reaction with each enzyme, unsulfated CXCR4 1−38 (peak a) was depleted and the different sulfation products appeared sequentially. Peak b was formed first in a relatively fast reaction. Only after peak a was almost completely converted to peak b were peaks c and d formed in parallel in a relatively slow second reaction step. Finally, peak e was formed as the end product of the sulfation reaction.

Although the overall rate of incorporation of sulfate into CXCR4 1−38 was similar for TPST-1 and TPST-2 (Figure 2F), we observed significant differences in the relative rates of formation and abundances of the various sulfation products. In particular, peak c was more abundant in the TPST-2-catalyzed sulfation reaction mixture than in the TPST-1-catalyzed reaction mixture.

Although a significant fraction of the peptide was fully sulfated after 160 h, the reaction was not complete with either TPST-1 or TPST-2. This incompleteness of the sulfation reaction can be attributed to the relatively slow rates of sulfation of Tyr-7 and Tyr-12. Furthermore, during the course of the in vitro sulfation reaction, we observed a progressive decline in the overall sulfation rate (Figure 2F), which might be explained by a loss of TPST activity or by hydrolysis of the cosubstrate PAPS. Furthermore, it is also likely that the continuous buildup of PAP and sulfopeptides leads to product inhibition of the TPST reaction. Whatever the causes, from the incompleteness of the in vitro peptide sulfation reaction no clear-cut conclusion can be drawn regarding the completeness of the CXCR4 sulfation reaction in vivo.

Binding of CXCR4 1−38 Sulfotyrosine Peptides to SDF-1α. To determine how sequential sulfation of tyrosine residues affects the binding affinity of the N-terminus of CXCR4 for SDF-1α, we performed binding experiments monitoring NMR chemical shift perturbations of SDF-1α residues (Figure 4). Previously, we titrated [^{15}N/^{13}C]SDF-1α (50 μM) with unsulfated (P38, peak a) and Y21-monosulfated (sY21 P38, peak b) CXCR4 1−38, and we monitored these titrations by ^{15}N−^{1}H HSQC spectroscopy to identify amino acid residues that experienced chemical shift changes upon peptide binding (*23*) (Figure 4A). By fitting the chemical shift changes as a function of peptide concentration, we obtained apparent dissociation constants of 4.5 ± 2.2 and 1.3 ± 0.5 μM for P38 and sY21 P38, respectively (*23*) (Figure 4B,C). We reported only apparent K_d values because peptide binding to SDF-1α shifts the SDF-1α monomer−dimer equilibrium toward dimer, which prevented us from directly observing the microscopic binding constants (*23*). In this work, we titrated [^{15}N/^{13}C]SDF-1α (50 μM) with the fully

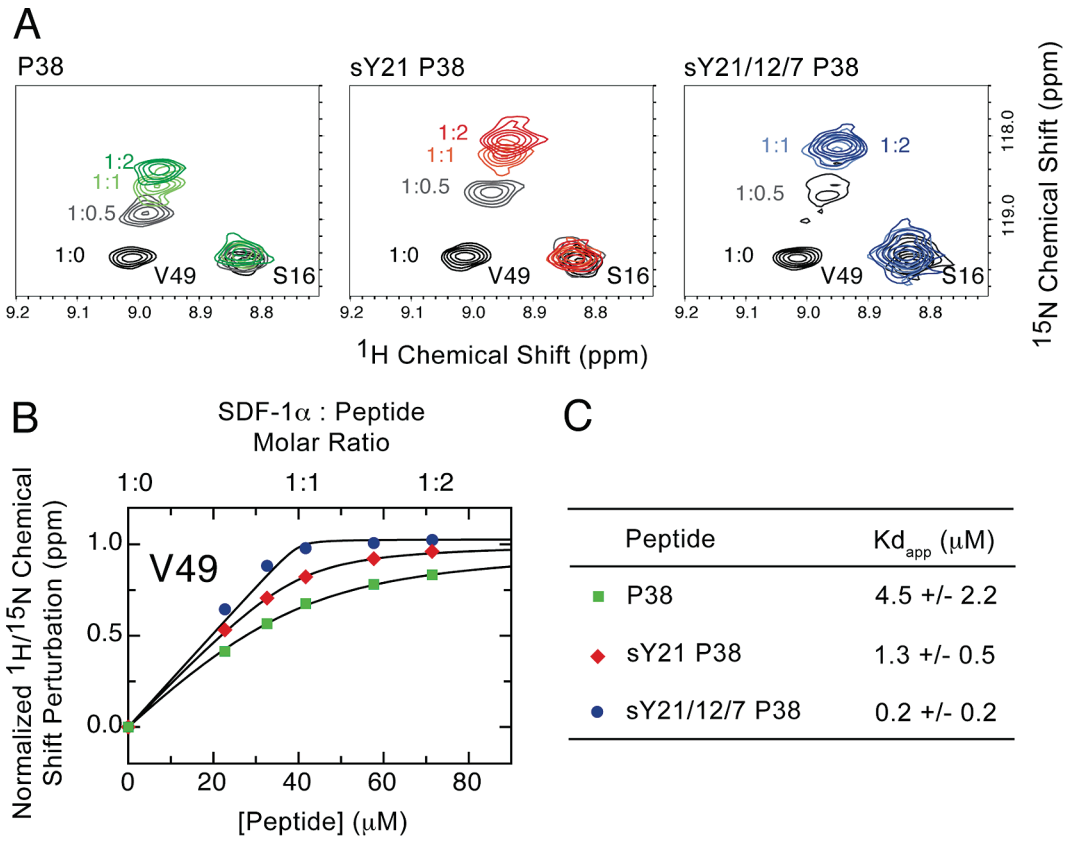

FIGURE 4: Effect of CXCR4 1−38 sulfation on the SDF-1α binding affinity. Apparent binding affinities were obtained by $^{15}N-^{1}H$ HSQC spectroscopy titrating ^{15}N- and ^{13}C-labeled SDF-1α with unsulfated (P38), Y21-monosulfated (sY21 P38), and fully sulfated (sY21/12/7 P38) CXCR4 1−38 peptides. (A) Overlaid portions of $^{15}N-^{1}H$ HSQC spectra of SDF-1α showing residue V49 during titration with P38, sY21 P38, and sY21/12/7 P38. SDF-1α:peptide ratios are 1:0 for black, 1:0.5 for gray, 1:1 for light green (P38), light red (sY21 P38), and light blue (sY21/12/7 P38), and 1:2 for green (P38), red (sY21 P38), and blue (sY21/12/7 P38) peaks. Only titration of SDF-1α with sY21/12/7 P38 resulted in saturation of SDF-1α chemical shift perturbations at a SDF-1α:peptide molar ratio of 1:1. (B) Normalized $^{1}H-^{15}N$ chemical shift perturbations for representative residue V49 of SDF-1α plotted vs peptide concentration for P38, sY21 P38 (data from ref*23*), and sY21/12/7 P38 (this study). For ease of comparison, maximum peptide-induced chemical shift perturbation for each titration was normalized to a value of 1. (C) Nonlinear curve fitting using titration data for SDF-1α residues 23, 25, 29, 31, 40−42, 47−51, 62, and 65−67 yielded apparent K_d values of 4.5 ± 2.2 μM for P38, 1.3 ± 0.5 μM for sY21 P38, and 0.2 ± 0.2 μM for sY21/12/7 P38.

triply sulfated peptide (sY21/12/7 P38, peak e) (Figure 4A,B) and derived an apparent peptide dissociation constant of 0.2 ± 0.2 μM (Figure 4C).

Figure 4A represents overlaid $^{15}N-^{1}H$ HSQC spectra of SDF-1α showing the chemical shift changes for residue V49 upon addition of P38, sY21 P38, or sY21/12/7 P38. Only titration of SDF-1α with sY21/12/7 P38 resulted in saturation of the chemical shift perturbations at a SDF-1α:peptide molar ratio of 1:1. Furthermore, when SDF-1α is titrated with sY21/12/7 P38, peak broadening in the $^{15}N-^{1}H$ HSQC spectra is observed at peptide ratios between 1:0 and 1:1 as seen for V49 at a SDF-1α:sY21/12/7 P38 ratio of 1:0.5 (Figure 4B). This peak broadening is indicative of a slower off rate corresponding to a higher affinity binding. Broad peaks in the $^{15}N-^{1}H$ HSQC spectra of SDF-1α titrated with P38 or sY21 P38 are not observed (Figure 4A). Figure 4B shows the combined ^{1}H and ^{15}N chemical shift changes for SDF-1α residue V49 when it is titrated with P38, sY21 P38, and sY21/12/7 P38. While the nearly stoichiometric binding of sY21/12/7 P38 to SDF-1α may not result in an accurate number for the fitted apparent K_d value, saturation of the ^{1}H and ^{15}N chemical shift change occurs much faster with sY21/12/7 P38, indicating that the fully sulfated N-terminal CXCR4 peptide has the highest affinity for SDF-1α binding of the three peptides. Taken together, these results show that sequential sulfation of the N-terminus of CXCR4 increases SDF-1α binding affinity, indicating a potential physiological role for sulfotyrosine residues at positions 21, 12, and 7.

DISCUSSION

Tyrosine sulfation is a widespread post-translational modification that is found in secreted and transmembrane proteins of multicellular organisms (*37*). In humans and mice, tyrosine sulfation is mediated by two isoenzymes, TPST-1 and TPST-2, which are located in the trans-Golgi network (*37, 38*). It has been estimated that up to 1% of all tyrosines of the eukaryotic proteome may be sulfated (*39*); however, the number of proteins that actually have been shown to contain sulfotyrosine residues is relatively small (*36, 37*). Among these are proteins important for hemostasis, chemotaxis, inflammation, and development, as well as proteins that are involved in viral and malaria infection and in cancer pathogenesis (*36, 37, 40*). Although the functional significance of tyrosine sulfation has been investigated in only a few systems, there is evidence that this modification may be an important modulator of extracellular protein−protein interactions (*36, 37, 40*).

Tyrosine sulfation of chemokine receptors and certain other GPCRs has been shown to enhance receptor−ligand

interactions. For example, sulfation of tyrosine residues in the N-terminus of chemokine receptor CCR5 is required for optimal chemokine receptor and HIV-1 coreceptor function (*41*−*44*). Likewise, tyrosine sulfation in the N-terminus of CXCR4 is also involved in the interaction with chemokine ligand SDF-1α (*23, 24*). However, and in contrast to CCR5, sulfotyrosine residues do not seem to be important for the interaction of HIV-1 gp120 with CXCR4 (*24*).

In most chemokine receptors and in many other sulfotyrosine proteins, multiple tyrosine residues that are potential sulfation sites are present (*36, 37, 40*). For example, the N-terminus of CCR5 contains four potential tyrosine sulfation sites (*25, 41*), while there are three such sites in the N-terminus of CXCR4 (*24*). For the majority of these multiple-sulfation sites, the tyrosine sulfation status is not well-defined. In particular, the extent to which the specific sites are sulfated in mature wild-type proteins and in the physiological context of cells that naturally express these sulfotyrosine proteins is not known. Furthermore, the specific contributions of individual sulfotyrosine residues to protein−protein interactions are also not well understood in most cases. These important questions cannot be answered using mutagenesis alone because amino acid replacements can affect sulfation at neighboring sites (*25, 41*) and because tyrosine sulfation might be limited by TPST activity in overexpression systems. Furthermore, the substrate specificity of the two known human TPSTs has not been determined, and sulfation efficiency at a specific site cannot be predicted because of the lack of a well-defined consensus sequence (*36, 37*).

To address these fundamental questions, we developed an in vitro sulfation assay using purified recombinant human TPST-1 (*26*) and TPST-2 (*27, 45*) to study tyrosine sulfation of peptide substrates containing multiple sulfation sites (*25*). By using this approach, we found that a peptide corresponding to the N-terminal region of CCR5 is sulfated by both TPST-1 and TPST-2, resulting in a final product in which all four tyrosine residues are sulfated (*25*). We also found that sulfates are added stepwise to the peptide and that Tyr-14 and Tyr-15 are sulfated first, followed by Tyr-10, and finally Tyr-3 (*25*).

Here we conducted a similar analysis using a peptide corresponding to amino acids 1−38 of CXCR4 as a model system to define the pattern and temporal sequence of tyrosine sulfation within the N-terminus of CXCR4. Furthermore, we used isolated sulfotyrosine peptide species in SDF-1α binding experiments to validate the physiological relevance of the observed in vitro sulfation sequence. Our results show that CXCR4 1−38 can be sulfated at similar overall rates by both TPST-1 and TPST-2, indicating that cellular sulfation of CXCR4 might not depend on a specific TPST isoenzyme. With both TPSTs, multiple sulfates (up to three) were incorporated into the CXCR4 1−38 peptide in a nonrandom, sequential fashion. Of the seven theoretically possible sulfotyrosine peptide species, only four were abundant in the in vitro sulfation assay. On the basis of the structures of the sulfation intermediates and the time course of the sulfation reaction, we concluded that Tyr-21 is sulfated first followed by Tyr-7 or Tyr-12. This apparent sulfation sequence is remarkably similar to the sequence observed with an N-terminal CCR5 peptide (*25*). In both cases, sulfation starts at the tyrosine(s) nearest the peptide C-terminus and proceeds in the direction of the N-terminus. It remains to be investigated whether this directionality represents a general preference of the TPST enzymes or if it is a common feature of the chemokine receptors.

There is no general consensus sequence for tyrosine sulfation. However, it has been shown that the information required for sulfation to occur is contained within five residues on either side of the tyrosine, and certain sequence elements have been identified that are common to known sulfation sites (*36, 37*). In particular, it has been shown that one or more acidic residues in the proximity of a tyrosine are required for sulfation to occur. We and others hypothesized on the basis of previous observations that within clusters of multiple sulfation sites sulfation of one site may depend on the negative charges of sulfates already present at other sites if the sites are separated by fewer than five amino acid residues (*25, 41*). Our results for CXCR4 1−38 indicate that both TPST-1 and TPST-2 have a strong site preference for sulfation of Tyr-21 over Tyr-7 and Tyr-12, which most likely reflects different intrinsic sulfation kinetics at these sites. Although sulfation at Tyr-7 and Tyr-12 is only observed after Tyr-21 is almost quantitatively sulfated, there is no evidence for a direct effect of a sulfotyrosine at position 21 on the intrinsic sulfation rates at the secondary sulfation sites. However, the reaction time courses for TPST-1- and TPST-2-catalyzed sulfation (Figure 2D,E) indicate that sulfation of either Tyr-7 or Tyr-12 might increase the rate of sulfation at the other site. Future sulfation studies using monosulfated (sTyr-21) or disulfated peptides (sTyr-21/7 and sTyr-21/12) as well as peptide variants lacking Tyr-21, -12, or -7 as substrates will be required to define precisely how the sulfation rate for each individual site might be affected by the sulfation status of the other two sites. Furthermore, future studies should also address whether N-glycosylation at Asn-11 and/or O-glycosylation at Ser-18 (*24*) might affect tyrosine sulfation of the N-terminus of CXCR4, because the fully processed glycan chains are already present when sulfation occurs in the trans-Golgi compartment (*38*).

Interestingly, computational tools such as "Sulfinator" (http://ca.expasy.org/tools/sulfinator/) and "Sulfosite" (http://sulfosite.mbc.nctu.edu.tw/) predict sulfation of Tyr-21 but fail to recognize Tyr-7 and Tyr-12 as potential sulfation sites. This inability of current computational methods to predict sulfation of unconventional sulfation sites emphasizes the need for highly sensitive analytical methods for studying tyrosine sulfation of proteins that are expressed at low levels and which contain clusters of potential sulfation sites (*36*).

Studies addressing the functional significance of tyrosine sulfation of CXCR4 have focused mainly on the role of sulfotyrosine 21 in the interaction with SDF-1α (*23, 24*). SDF-1α binding competition studies with CXCR4 mutants indicated that sulfation of Tyr-21 is required for high-affinity interaction with SDF-1α (*24*). Furthermore, NMR spectroscopy studies using Tyr-21 monosulfated CXCR4 peptides identified a putative binding site for sulfotyrosine 21 on SDF-1α that includes Arg-47, suggesting the formation of a salt bridge between Arg-47 and sulfotyrosine 21 (*23*). The possible involvement of sulfotyrosines at positions 7 and 12 could not be addressed in these studies because Tyr-7 and Tyr-12 are not efficiently sulfated in heterologously ex-

pressed CXCR4 mutants (*24*) and fully sulfated CXCR4 peptides have not been available. Our in vitro sulfation results demonstrate that, in principle, both human TSPTs are capable of quantitatively modifying all three potential sulfation sites in the N-terminus of CXCR4. They also provide an enzymatic explanation for the inefficient sulfation of Tyr-7 and Tyr-12 observed in CXCR4 mutants (*24*). Furthermore, the SDF-1α binding results show that the fully sulfated N-terminus of CXCR4 binds SDF-1α with higher affinity than the unsulfated or monosulfated N-terminus of CXCR4, indicating a potential functional role for sulfation of Tyr-7 and/or Tyr-12.

More recently, using the improved tyrosine sulfation methods described in this paper, we were able to solve the solution NMR structures of a dimeric SDF-1α variant in complex with CXCR4 1−38 peptides containing none, one (sTyr-21), or three sulfotyrosine residues (sTyr-7,12,21) (*46*). These structures confirm that SDF-1α residue Arg-47 is directly involved in a binding interaction with sulfotyrosine 21. Furthermore, the structures also show that if sulfotyrosines are present at positions 7 and 12, they interact with SDF-1α residues Arg-20 and Lys-27, respectively. Interestingly, because the bound CXCR4 peptide bridges the SDF-1α dimer interface, sulfotyrosine residues 21 and 12 interact with residues Arg-47 and Lys-27 on one subunit, whereas sulfotyrosine-7 interacts with residue Arg-20 on the other subunit. The interaction site of sulfotyrosine 7 in a complex with monomeric SDF-1α is currently not known.

Taken together, our results strongly suggest that sulfotyrosines at positions 7 and 12, if present, will enhance the interaction of CXCR4 with SDF-1α. It is tempting to speculate that incomplete sulfation of these sites in CXCR4, or similar sites in other chemokine receptors such as CCR5, might play a physiological role by creating a heterogeneous ensemble of chemokine receptor molecules with different affinities for a given chemokine agonist. Such a heterogeneous ensemble of receptor molecules would allow a migrating cell to respond to an extended range of concentrations within a chemokine gradient and, in particular, might alter the chemotactic response at the lower end of the concentration−response curve. Further studies will be required to precisely define the sulfation status of CXCR4 in the context of cells which naturally express this receptor and to clarify the functional significance of heterogeneous receptor sulfation under experimental conditions that more closely resemble the physiological situation in vivo.

Sulfotyrosine peptides are valuable tools for studying protein−protein interactions involving recognition of specific sulfotyrosine residues. For example, glycosulfopeptides corresponding to the N-terminus of PSGL-1 have been used to characterize the interaction between PSGL-1 and P-selectin (*47, 48*). Furthermore, we and others have used sulfotyrosine peptides corresponding to the N-termini of CCR5 and CXCR4 to study the interaction of the chemokine receptors with HIV-1 gp120 (*42, 43, 49*−*51*) and with the chemokine ligands (*23, 43, 50, 52*). Chemical methods for the synthesis of sulfated peptides exist (see ref*36* and references cited therein); however, the sensitivity of the tyrosine sulfoester bond to strong acids tends to result in low overall yields, and peptides with multiple sulfotyrosines are generally difficult to obtain. We and others have demonstrated that enzymatic sulfation is a useful alternative to the chemical synthesis of sulfotyrosine peptides (*23, 25, 36, 48*). In the past, chemoenzymatic synthesis of sulfotyrosine peptides has been limited by the low yields and high costs of TPST expression in mammalian cell lines. However, these problems have been overcome by recent progress in obtaining large quantities of functional TPSTs from *E. coli* expression systems (C. Seibert and T. P. Sakmar, manuscript in preparation). Alternatively, Liu et al. (*53*) demonstrated that sulfotyrosine peptides and proteins can also be obtained by recombinant expression in *E. coli* using the amber suppression method to site specifically incorporate sulfotyrosine residues as unnatural amino acids.

In summary, this study provides a detailed analysis of the multiple-sulfation reaction of a TPST peptide substrate corresponding to the N-terminal region of chemokine receptor CXCR4. The methods developed will be useful for exploring the chemokine receptor sulfoproteome and for the preparation of sulfotyrosine peptides for structural and functional studies of chemokine receptor signaling. These results provide a basis for understanding the enzymology of TPST-mediated CXCR4 sulfation in the trans-Golgi compartment and for understanding the role of specific sulfotyrosine residues in chemokine recognition.

ACKNOWLEDGMENT

We thank Dr. Kevin L. Moore (University of Oklahoma Health Sciences Center) for providing the TPST expression vectors, Dr. Martine Cadene (CNRS, Orleans, France) for valuable discussions, and Dr. Haiteng Deng (Proteomics Core Facility, The Rockefeller University) for access to mass spectrometry equipment.

REFERENCES

1. Bleul, C. C., Farzan, M., Choe, H., Parolin, C., Clark-Lewis, I., Sodroski, J., and Springer, T. A. (1996) The lymphocyte chemoattractant SDF-1 is a ligand for LESTR/fusin and blocks HIV-1 entry. *Nature 382*, 829–833.
2. Oberlin, E., Amara, A., Bachelerie, F., Bessia, C., Virelizier, J. L., Arenzana-Seisdedos, F., Schwartz, O., Heard, J. M., Clark-Lewis, I., Legler, D. F., Loetscher, M., Baggiolini, M., and Moser, B. (1996) The CXC chemokine SDF-1 is the ligand for LESTR/fusin and prevents infection by T-cell-line-adapted HIV-1. *Nature 382*, 833–835.
3. Murphy, P. M., Baggiolini, M., Charo, I. F., Hebert, C. A., Horuk, R., Matsushima, K., Miller, L. H., Oppenheim, J. J., and Power, C. A. (2000) International union of pharmacology. XXII. Nomenclature for chemokine receptors. *Pharmacol. Rev. 52*, 145–176.
4. Loetscher, M., Geiser, T., O'Reilly, T., Zwahlen, R., Baggiolini, M., and Moser, B. (1994) Cloning of a human seven-transmembrane domain receptor, LESTR, that is highly expressed in leukocytes. *J. Biol. Chem. 269*, 232–237.
5. Feng, Y., Broder, C. C., Kennedy, P. E., and Berger, E. A. (1996) HIV-1 entry cofactor: Functional cDNA cloning of a seven-transmembrane, G protein-coupled receptor. *Science 272*, 872–877.
6. Proudfoot, A. E. (2002) Chemokine receptors: Multifaceted therapeutic targets. *Nat. Rev. Immunol. 2*, 106–115.
7. Nagasawa, T., Hirota, S., Tachibana, K., Takakura, N., Nishikawa, S., Kitamura, Y., Yoshida, N., Kikutani, H., and Kishimoto, T. (1996) Defects of B-cell lymphopoiesis and bone-marrow myelopoiesis in mice lacking the CXC chemokine PBSF/SDF-1. *Nature 382*, 635–638.
8. Tachibana, K., Hirota, S., Iizasa, H., Yoshida, H., Kawabata, K., Kataoka, Y., Kitamura, Y., Matsushima, K., Yoshida, N., Nishikawa, S., Kishimoto, T., and Nagasawa, T. (1998) The chemokine receptor CXCR4 is essential for vascularization of the gastrointestinal tract. *Nature 393*, 591–594.

9. Zou, Y. R., Kottmann, A. H., Kuroda, M., Taniuchi, I., and Littman, D. R. (1998) Function of the chemokine receptor CXCR4 in haematopoiesis and in cerebellar development. *Nature 393*, 595–599.
10. Muller, A., Homey, B., Soto, H., Ge, N., Catron, D., Buchanan, M. E., McClanahan, T., Murphy, E., Yuan, W., Wagner, S. N., Barrera, J. L., Mohar, A., Verastegui, E., and Zlotnik, A. (2001) Involvement of chemokine receptors in breast cancer metastasis. *Nature 410*, 50–56.
11. Scotton, C. J., Wilson, J. L., Milliken, D., Stamp, G., and Balkwill, F. R. (2001) Epithelial cancer cell migration: A role for chemokine receptors? *Cancer Res. 61*, 4961–4965.
12. Scotton, C. J., Wilson, J. L., Scott, K., Stamp, G., Wilbanks, G. D., Fricker, S., Bridger, G., and Balkwill, F. R. (2002) Multiple actions of the chemokine CXCL12 on epithelial tumor cells in human ovarian cancer. *Cancer Res. 62*, 5930–5938.
13. Rubin, J. B., Kung, A. L., Klein, R. S., Chan, J. A., Sun, Y., Schmidt, K., Kieran, M. W., Luster, A. D., and Segal, R. A. (2003) A small-molecule antagonist of CXCR4 inhibits intracranial growth of primary brain tumors. *Proc. Natl. Acad. Sci. U.S.A. 100*, 13513–13518.
14. Berger, E. A., Murphy, P. M., and Farber, J. M. (1999) Chemokine receptors as HIV-1 coreceptors: Roles in viral entry, tropism, and disease. *Annu. Rev. Immunol. 17*, 657–700.
15. Zhang, Y., Lou, B., Lal, R. B., Gettie, A., Marx, P. A., and Moore, J. P. (2000) Use of inhibitors to evaluate coreceptor usage by simian and simian/human immunodeficiency viruses and human immunodeficiency virus type 2 in primary cells. *J. Virol. 74*, 6893–6910.
16. Zhang, Y. J., and Moore, J. P. (1999) Will multiple coreceptors need to be targeted by inhibitors of human immunodeficiency virus type 1 entry? *J. Virol. 73*, 3443–3448.
17. de Roda Husman, A. M., and Schuitemaker, H. (1998) Chemokine receptors and the clinical course of HIV-1 infection. *Trends Microbiol. 6*, 244–249.
18. Douek, D. C., Picker, L. J., and Koup, R. A. (2003) T cell dynamics in hiv-1 infection. *Annu. Rev. Immunol. 21*, 265–304.
19. Brelot, A., Heveker, N., Montes, M., and Alizon, M. (2000) Identification of residues of CXCR4 critical for human immunodeficiency virus coreceptor and chemokine receptor activities. *J. Biol. Chem. 275*, 23736–23744.
20. Zhou, N., Luo, Z., Luo, J., Liu, D., Hall, J. W., Pomerantz, R. J., and Huang, Z. (2001) Structural and functional characterization of human CXCR4 as a chemokine receptor and HIV-1 co-receptor by mutagenesis and molecular modeling studies. *J. Biol. Chem. 276*, 42826–42833.
21. Doranz, B. J., Orsini, M. J., Turner, J. D., Hoffman, T. L., Berson, J. F., Hoxie, J. A., Peiper, S. C., Brass, L. F., and Doms, R. W. (1999) Identification of CXCR4 domains that support coreceptor and chemokine receptor functions. *J. Virol. 73*, 2752–2761.
22. Crump, M. P., Gong, J. H., Loetscher, P., Rajarathnam, K., Amara, A., Arenzana-Seisdedos, F., Virelizier, J. L., Baggiolini, M., Sykes, B. D., and Clark-Lewis, I. (1997) Solution structure and basis for functional activity of stromal cell- derived factor-1: Dissociation of CXCR4 activation from binding and inhibition of HIV-1. *EMBO J. 16*, 6996–7007.
23. Veldkamp, C. T., Seibert, C., Peterson, F. C., Sakmar, T. P., and Volkman, B. F. (2006) Recognition of a CXCR4 sulfotyrosine by the chemokine stromal cell-derived factor-1α (SDF-1α/CXCL12). *J. Mol. Biol. 359*, 1400–1409.
24. Farzan, M., Babcock, G. J., Vasilieva, N., Wright, P. L., Kiprilov, E., Mirzabekov, T., and Choe, H. (2002) The role of post-translational modifications of the CXCR4 amino-terminus in SDF-1a association and HIV-1 entry. *J. Biol. Chem. 277*, 29484–29489.
25. Seibert, C., Cadene, M., Sanfiz, A., Chait, B. T., and Sakmar, T. P. (2002) Tyrosine sulfation of CCR5 N-terminal peptide by tyrosylprotein sulfotransferases 1 and 2 follows a discrete pattern and temporal sequence. *Proc. Natl. Acad. Sci. U.S.A. 99*, 11031–11036.
26. Ouyang, Y. B., Lane, W. S., and Moore, K. L. (1998) Tyrosylprotein sulfotransferase: Purification and molecular cloning of an enzyme that catalyzes tyrosine O-sulfation, a common posttranslational modification of eukaryotic proteins. *Proc. Natl. Acad. Sci. U.S.A. 95*, 2896–2901.
27. Ouyang, Y. B., and Moore, K. L. (1998) Molecular cloning and expression of human and mouse tyrosylprotein sulfotransferase-2 and a tyrosylprotein sulfotransferase homologue in *Caenorhabditis elegans*. *J. Biol. Chem. 273*, 24770–24774.
28. Pennings, E. J. M., and van Kempen, G. M. J. (1979) Analysis of 3′-phophoadenylylsulphate and related compounds by paired-ion high-performance liquid chromatography. *J. Chromatogr. 176*, 478–479.
29. Burkart, M. D., Izumi, M., Chapman, E., Lin, C. H., and Wong, C. H. (2000) Regeneration of PAPS for the enzymatic synthesis of sulfated oligosaccharides. *J. Org. Chem. 65*, 5565–5574.
30. *Specifications and Criteria for Biochemical Compounds* (1972) 3rd ed., p 159, National Academy of Sciences, Washington, DC.
31. Cadene, M., and Chait, B. T. (2000) A robust, detergent-friendly method for mass spectrometric analysis of integral membrane proteins. *Anal. Chem. 72*, 5655–5658.
32. Karas, M., and Hillenkamp, F. (1988) Laser desorption ionization of proteins with molecular masses exceeding 10,000 daltons. *Anal. Chem. 60*, 2299–2301.
33. Beavis, R. C., and Chait, B. T. (1996) Matrix-assisted laser desorption ionization mass-spectrometry of proteins. *Methods Enzymol. 270*, 519–551.
34. Veldkamp, C. T., Peterson, F. C., Pelzek, A. J., and Volkman, B. F. (2005) The monomer-dimer equilibrium of stromal cell-derived factor-1 (CXCL 12) is altered by pH, phosphate, sulfate, and heparin. *Protein Sci. 14*, 1071–1081.
35. Gozansky, E. K., Louis, J. M., Caffrey, M., and Clore, G. M. (2005) Mapping the binding of the N-terminal extracellular tail of the CXCR4 receptor to stromal cell-derived factor-1α. *J. Mol. Biol. 345*, 651–658.
36. Seibert, C., and Sakmar, T. P. (2008) Toward a framework for sulfoproteomics: Synthesis and characterization of sulfotyrosine-containing peptides. *Biopolymers 90*, 459–477.
37. Moore, K. L. (2003) The biology and enzymology of protein tyrosine O-sulfation. *J. Biol. Chem. 278*, 24243–24246.
38. Baeuerle, P. A., and Huttner, W. B. (1987) Tyrosine sulfation is a trans-Golgi-specific protein modification. *J. Cell Biol. 105*, 2655–2664.
39. Baeuerle, P. A., and Huttner, W. B. (1986) Chlorate: A potent inhibitor of protein sulfation in intact cells. *Biochem. Biophys. Res. Commun. 141*, 870–877.
40. Kehoe, J. W., and Bertozzi, C. R. (2000) Tyrosine sulfation: A modulator of extracellular protein-protein interactions. *Chem. Biol. 7*, R57−R61.
41. Farzan, M., Mirzabekov, T., Kolchinsky, P., Wyatt, R., Cayabyab, M., Gerard, N. P., Gerard, C., Sodroski, J., and Choe, H. (1999) Tyrosine sulfation of the amino terminus of CCR5 facilitates HIV-1 entry. *Cell 96*, 667–676.
42. Cormier, E. G., Persuh, M., Thompson, D. A., Lin, S. W., Sakmar, T. P., Olson, W. C., and Dragic, T. (2000) Specific interaction of CCR5 amino-terminal domain peptides containing sulfotyrosines with HIV-1 envelope glycoprotein gp120. *Proc. Natl. Acad. Sci. U.S.A. 97*, 5762–5767.
43. Farzan, M., Vasilieva, N., Schnitzler, C. E., Chung, S., Robinson, J., Gerard, N. P., Gerard, C., Choe, H., and Sodroski, J. (2000) A tyrosine-sulfated peptide based on the N terminus of CCR5 interacts with a CD4-enhanced epitope of the HIV-1 gp120 envelope glycoprotein and inhibits HIV-1 entry. *J. Biol. Chem. 275*, 33516–33521.
44. Bannert, N., Craig, S., Farzan, M., Sogah, D., Santo, N. V., Choe, H., and Sodroski, J. (2001) Sialylated O-glycans and sulfated tyrosines in the NH2-terminal domain of CC chemokine receptor 5 contribute to high affinity binding of chemokines. *J. Exp. Med. 194*, 1661–1673.
45. Beisswanger, R., Corbeil, D., Vannier, C., Thiele, C., Dohrmann, U., Kellner, R., Ashman, K., Niehrs, C., and Huttner, W. B. (1998) Existence of distinct tyrosylprotein sulfotransferase genes: Molecular characterization of tyrosylprotein sulfotransferase-2. *Proc. Natl. Acad. Sci. U.S.A. 95*, 11134–11139.
46. Veldkamp, C. T., Seibert, C., Peterson, F. C., De la Cruz, N., Haugner, J. C., Basnet, H., Sakmar, T. P., and Volkman, B. F. (2008) Structural Basis of CXCR4 Sulfotyrosine Recognition by the Chemokine SDF-1. *Sci. Signal. 1*, ra4.
47. Somers, W. S., Tang, J., Shaw, G. D., and Camphausen, R. T. (2000) Insights into the molecular basis of leukocyte tethering and rolling revealed by structures of P- and E-selectin bound to SLe(X) and PSGL-1. *Cell 103*, 467–479.
48. Leppanen, A., Mehta, P., Ouyang, Y. B., Ju, T., Helin, J., Moore, K. L., van Die, I., Canfield, W. M., McEver, R. P., and Cummings, R. D. (1999) A novel glycosulfopeptide binds to P-selectin and inhibits leukocyte adhesion to P-selectin. *J. Biol. Chem. 274*, 24838–24848.

49. Cormier, E. G., Tran, D. N., Yukhayeva, L., Olson, W. C., and Dragic, T. (2001) Mapping the determinants of the CCR5 amino-terminal sulfopeptide interaction with soluble human immunodeficiency virus type 1 gp120-CD4 complexes. *J. Virol. 75*, 5541–5549.
50. Farzan, M., Chung, S., Li, W., Vasilieva, N., Schnitzler, C. E., Marchione, R. J., Gerard, C., Gerard, N. P., Sodroski, J., and Choe, H. (2002) Tyrosine-sulfated peptides functionally reconstitute a CCR5 variant lacking a critical amino-terminal region. *J. Biol. Chem. 277*, 40397–40402.
51. Huang, C. C., Lam, S. N., Acharya, P., Tang, M., Xiang, S. H., Hussan, S. S., Stanfield, R. L., Robinson, J., Sodroski, J., Wilson, I. A., Wyatt, R., Bewley, C. A., and Kwong, P. D. (2007) Structures of the CCR5 N terminus and of a tyrosine-sulfated antibody with HIV-1 gp120 and CD4. *Science 317*, 1930–1934.
52. Duma, L., Haussinger, D., Rogowski, M., Lusso, P., and Grzesiek, S. (2007) Recognition of RANTES by Extracellular Parts of the CCR5 Receptor. *J. Mol. Biol. 365*, 1063–1075.
53. Liu, C. C., and Schultz, P. G. (2006) Recombinant expression of selectively sulfated proteins in *Escherichia coli*. *Nat. Biotechnol. 24*, 1436–1440.

BI800965M